J. Cell. Mol. Med. Vol 14, No 7, 2010 pp. 1962-1974

Cell cloning-based transcriptome analysis in Rett patients: relevance to the pathogenesis of Rett syndrome of new human MeCP2 target genes

J. Nectoux [a, b, c], Y. Fichou [a, b], H. Rosas-Vargas [a, b], N. Cagnard [d], N. Bahi-Buisson [e], P. Nusbaum [c], F. Letourneur [a, b], J. Chelly [a, b, c], T. Bienvenu [a, b, c, *]

[a] *Genetics and Pathophysiology of Neurodevelopmental and Nueromuscular Disorders Department, Cochin Institute, Paris Descartes University, Paris, France*
[b] *Institut National de la Santé et de la Recherche Médicale (INSERM), Paris, France*
[c] *Assistance Publique – Hôpitaux de Paris, Cochin Hospital, Biochemical and Molecular Genetics Laboratory, Paris, France*
[d] *Bioinformatics Platform, Paris Descartes University, Paris, France*
[e] *Assistance Publique – Hôpitaux de Paris, Necker-Enfants Malades Hospital, Pediatric Neurology, Paris, France*

Received: August 1, 2008; Accepted: April 27, 2009

Abstract

More than 90% of Rett syndrome (RTT) patients have heterozygous mutations in the X-linked methyl-CpG binding protein 2 (*MECP2*) gene that encodes the methyl-CpG-binding protein 2, a transcriptional modulator. Because *MECP2* is subjected to X chromosome inactivation (XCI), girls with RTT either express the wild-type or mutant allele in each individual cell. To test the consequences of *MECP2* mutations resulting from a genome-wide transcriptional dysregulation and to identify its target genes in a system that circumvents the functional mosaicism resulting from XCI, we carried out gene expression profiling of clonal populations derived from fibroblast primary cultures expressing exclusively either the wild-type or the mutant *MECP2* allele. Clonal cultures were obtained from skin biopsy of three RTT patients carrying either a non-sense or a frameshift *MECP2* mutation. For each patient, gene expression profiles of wild-type and mutant clones were compared by oligonucleotide expression microarray analysis. Firstly, clustering analysis classified the RTT patients according to their genetic background and *MECP2* mutation. Secondly, expression profiling by microarray analysis and quantitative RT-PCR indicated four up-regulated genes and five down-regulated genes significantly dysregulated in all our statistical analysis, including excellent potential candidate genes for the understanding of the pathophysiology of this neurodevelopmental disease. Thirdly, chromatin immunoprecipitation analysis confirmed MeCP2 binding to respective CpG islands in three out of four up-regulated candidate genes and sequencing of bisulphite-converted DNA indicated that MeCP2 preferentially binds to methylated-DNA sequences. Most importantly, the finding that at least two of these genes (*BMCC1* and *RNF182*) were shown to be involved in cell survival and/or apoptosis may suggest that impaired MeCP2 function could alter the survival of neurons thus compromising brain function without inducing cell death.

Keywords: MeCP2 • transcriptome • Rett syndrome

Introduction

The postnatal, neurodevelopmental disorder Rett syndrome (RTT, MIM 312750) is caused by mutations in the gene encoding the methyl-CpG binding protein 2 (MeCP2) [1]. *MECP2* mutations have been identified in approximately 90% of classical RTT patients. This genetic disease is characterized by a postnatal, normal development for the first few months followed by developmental stagnation and regression, loss of purposeful hand movements and speech, truncal ataxia, stereotypic hand movements, deceleration of brain growth, autonomic dysfunction and seizures [2].

MeCP2 is a member of the methyl-CpG binding protein family, and is composed by three domains: the methyl-binding domain (MBD), the transcriptional repression domain and a C-terminal

*Correspondence to: Thierry BIENVENU,
Institut Cochin, Laboratoire de Génétique des Maladies Neurodéveloppementales, CHU Cochin – 24 Rue du Faubourg Saint Jacques, 75014 Paris, France
Tel.: +33 1 44 41 24 79
Fax: +33 1 44 41 24 21
E-mail: thierry.bienvenu@inserm.fr

doi:10.1111/j.1582-4934.2010.01107.x

domain, in addition to two nuclear localization signals. The MBD specifically binds to methylated CpG dinucleotides, with higher affinity for CpG sequences with adjacent A/T-rich motifs [3], but also binds to unmethylated four-way DNA junctions with a similar affinity, indicating a role of MeCP2 in higher-order chromatin interaction [2]. The function of MeCP2 as a transcriptional repressor was first suggested based on *in vitro* experiments. It was shown to specifically inhibit transcription of genes with methylated promoters after binding to methylated CpG dinucleotides *via* its MBD, and recruiting the corepressor Sin3A and histone deacetylases 1 and 2 by its transcriptional repression domain [4, 5]. The transcriptional repressor activity of MeCP2 involves the compaction of chromatin by promoting nucleosome clustering, either through the recruitment of histone deacetylase and histone deacetylation or through a direct interaction between its C-terminal domain and chromatin. However, recent studies suggest that MeCP2 regulates the expression of a wide range of genes and that it can both repress and activate transcription [6, 7].

Given that RTT may likely result from dysfunction of a putative transcriptional modulator activity of MeCP2, several groups have developed strategies to identify the transcriptional targets of MeCP2 in order to gain insights into the disease pathogenesis. Transcriptional profiling studies using brain tissue from Mecp2-null mice did not reveal major changes in gene expression, suggesting that MeCP2 may not be a global transcriptional repressor as previously thought, and that loss of MeCP2 function leads to subtle gene expression variations [8]. However, a recent study using hypothalamus tissues from Mecp2-null mice and Mecp2-transgenic mice showed that more than 2100 genes are misregulated in both mouse models, although the magnitude of the changes in expression levels for both activated and repressed genes was moderate [6]. Several studies have also used the candidate gene approach in samples from both human and mouse tissues, and identified putative MeCP2 targets that might be relevant to the pathogenesis of RTT [9–12]. Some of these targets, such as the brain-derived neurotrophic factor and the phospholemman precursor (*FXYD1*) have been confirmed, mainly in mice models, while others, such as *DLX5* and *UBE3A*, were found inconsistently differentially expressed [13–14]. In the present study, we bypassed some of the limitations of expression profiling on unavailable or complex tissues, such as brain, as well as those of transformed lymphoblastoid cell lines, by studying clonal cultures of non-transformed fibroblasts derived from RTT patients. These cells were obtained by skin biopsy, readily cultured and subjected to single-cell subcloning. Because *MECP2* undergoes X chromosome inactivation (XCI), cells expressing the wild-type *MECP2* gene can be clonally separated from those that express the mutant transcript. A similar approach has already been performed with fibroblast strains from Coriell Cell repositories carrying different classes of mutations (such as missense and frameshift mutations) [15]. To identify downstream MeCP2 targets, we compared the global gene expression patterns in matched pairs of clonally derived mutant or wild-type *MECP2*-expressing fibroblast cultures from three unrelated RTT girls carrying only mutations leading to premature stop codon. Our expression profiling by microarray analysis and quantitative RT-PCR revealed, in all our statistical analysis, nine genes with significant differential expression.

Materials and methods

Cell culture, single cell cloning and nucleic acid extraction for fibroblasts

After informed consent obtained from the parents, a skin biopsy was carried out on three girls suffering from typical RTT. Clonal cultures were obtained from primary cultures of human fibroblasts by the limit dilution method. Briefly, fibroblasts from the patients were plated at equivalent one cell in 96-well plates in Dulbecco's modified Eagle's medium F-12 HAM (Sigma-Aldrich Chimie, Lyon, France) supplemented with 10% heat-inactivated foetal bovine serum and 50 units/ml penicillin and streptomycin. All cultures were routinely grown at 37°C, 5% CO_2 in a humidified atmosphere. Wells indicating positive growth were systematically tested for clonality by three independent, complementary cellular and molecular approaches: allele-specific transcript analysis, XCI study and immunocytochemical analysis with MeCP2 antibody. Total RNA was extracted from fibroblast clones with the Qiagen RNeasy kit (Qiagen, Courtaboeuf, France) as described by the manufacturer. Prior to array hybridization, RNA quality was assessed with the Agilent 2100 Bioanalyzer (Agilent Technologies, Massy, France). DNA was extracted using a standard extraction protocol to determine XCI status and to check their clonal status.

Allele-specific transcript analysis

After DNase I digestion (Roche Diagnostics, Meylan, France), reverse transcription of total RNA (1 μg/reaction) was carried out with the Superscript™ II RNase H-Reverse Transcriptase (Invitrogen, Cergy-Pontoise, France) using 500 ng of random hexamers. Regions containing the mutations were amplified by PCR (Table 1) and sequenced with an ABI 3100® (Applied Biosystems, Courtaboeuf, France). Cell clones expressing only the normal *MECP2* allele are called 'wild-type clones', while cell clones or skewed cell lines expressing only the mutant *MECP2* allele are called 'mutant clones'.

X chromosome inactivation study

XCI status was investigated by sizing the polymorphic CAG trinucleotide repeat on the inactive androgen receptor allele [16]. Digestion of four restriction sites located between the flanking primers and adjacent to the trinucleotide repeat were carried out with the methylation sensitive enzymes HpaII and CfoI. Amplification of the undigested allele including the trinucleotide repeat region was performed with the fluorescent-labelled, forward primer 5′-FAM-TGCGCGAAGTGATCCAGAAC-3′, and the unlabelled, reverse primer 5′-CTTGCGGAGAACCATCCTCA-3′. Amplification products were sized with the ABI 3100® sequencer using GeneScan™ Fragment Analysis software (Applied Biosystems). Undigested DNA samples of each original cell culture were amplified to size each allele.

Table 1 Primer sequences for the amplification by RT-PCR and direct sequencing of *MECP2* mutations. bp: base pairs; Ta: annealing temperature

	Oligonucleotide sequence (5′-3′)	PCR size (bp)	PCR Ta (°C)
Patient 1, p.R255X,			
Patient 2, p.R270X	CCTGAAGGCTGGACACGGAAGC	701	60
	CTTTCCCGCTCTTCTCACCG		
Patient 3, p.L386fs	CCTGAAGGCTGGACACGGAAGC	934	60
	AGACGCTGCTGCTCAAGTCC		

Immunocytochemical analysis with MeCP2 antibody

MeCP2 protein expression in fibroblasts was determined by immunofluorescence analysis as previously described [17]. Antibodies were directed against the N-terminal domain (amino acids 6–25) (PAI-887, ABR, Ozyme, St-Quentin-En-Yvelines, France), and the C-terminal domain (amino acids 465–478) (M9317, Sigma, Lyon, France).

Cells were fixed with 4% paraformaldehyde for 20 min., mounted with Vectashield mounting medium with DAPI (Vector Laboratories, purchased from Abcys, Paris, France) and analysed with a Leica DMRA2 fluorescence microscope (Leica, Nanterre, France).

Microarray data analysis

Total RNA from each selected clonal culture was analysed with the Affymetrix Human Genome HGU133 Plus 2.0 Chips (a genome-wide array with 54,674 probe sets). RNA was scanned for purity, quality and amount with an Agilent 2100 Bioanalyzer using the RNA 6000 Nano LabChip®. When the 18S/28S ratio was ~2.0, total RNA was subjected to subsequent labelling and cDNA synthesis for hybridization was carried out with 2 μg of total RNA and standard Affymetrix kits (Affymetrix, High Wycombe, UK). cDNA was washed with the Affymetrix cDNA cleanup kit. *In vitro* transcription and labelling of cRNA were performed with Affymetrix reagents designed for *in vitro* transcription, amplification and biotin-labelling to generate targets for GeneChip® brand arrays. Hybridization was carried out according to the Affymetrix GeneChip® Manual. Fifteen micrograms of labelled, fragmented *in vitro* transcription material was the nominal amount used on the GeneChip® arrays. The arrays were incubated overnight at a constant 45°C temperature. Preparation of microarrays was carried out with Affymetrix wash protocols in a Model 450 Fluidics station under the control of Affymetrix GeneChip Operating Software. Scanning was carried out with an Affymetrix Model 3000 scanner with an autoloader.

Fluorescent data were exported to two complementary analysis packages: (1) Genespring software (Agilent Technologies) with GC-RMA (robust multichip average) algorithm for data normalization and (2) R Bioconductor with the RMA module with MAS5.0 algorithm for data filtering (http://www.r-project.org/). Normalization by Genespring GC-RMA allows a model-based probe-specific background correction to maintain accuracy even for very low expressed genes [18]. MAS5.0 detection flags allow accuracy in signal quality filtering. It generates a *P*-score that assesses the reliability of each expression level, considering the significance of the differences between the perfect match and the mismatch values for each probeset. One of the following flag: 'absent', 'marginal' or 'present' is associated to each probe pair according to the strength of the fluorescent signal. Three probe lists were used for each comparison according to flagged measurement in the relevant chips. The 'PP' list is made of probes only flagged as 'Present' for all chips involved in the comparison. The 'P50' list has been created by filtering the probes flagged as 'Present' for at least half of the chips. The 'All' list is made of all probes without any filter. For statistical analyses, differences in gene expression level between wild-type and mutant clones for each patient (matched pairs) were calculated, and difference in means was first tested by paired t-test. Secondly, we compared all mutant clones to all wild-type clones without considering them as pairs by unpaired t-test. To estimate the false discovery rate, the resulting *P*-values were filtered at 5% and corrected by the Benjamini and Hochberg method. Cluster analysis was performed by hierarchical clustering in Genespring using the Spearman correlation similarly measure and average linkage algorithm.

Chromatin immunoprecipitation (ChIP)

Chromatin of a primary culture of human MeCP2 wild-type fibroblasts was extracted with the ChIP-IT™ Express kit (Active Motif, Rixensart, Belgium) according to the manufacturer's instructions. Briefly, three 15 cm^2 tissue culture dishes of fibroblasts at 80–90% confluency (~4×10^7 cells) were cross-linked with a 1% formaldehyde-DMEM solution at room temperature for 10 min. under gently agitation. Fixation was stopped with a 1% glycine-PBS 1X solution. Cells were rinsed, scraped off the plates and collected by centrifugation, 720 × *g*, 10 min., 4°C in ice-cold PBS 1X supplemented with 0.5 mM PMSF. The pellet was resuspended in lysis buffer supplemented with PMSF and protease inhibitor cocktail and incubated on ice for 30 min. Cells were gently dounced on ice with 10 strokes to release the nuclei and centrifuged at 2400 × *g*, 10 min., 4°C to pellet the nuclei. The pellet was resuspended in shearing buffer supplemented with protease inhibitor

Table 2 Primer sequences and amplicon size for the amplification of putative MeCP2 targets from ChIP-isolated chromatin and bisulphite-converted DNA. bp: base pairs; Ta: annealing temperature. PCR amplifications at Ta 60°C were performed with an additional buffer (PCRx Enhancer System1X, Invitrogen)

Gene	Forward primer sequence	Reverse primer sequence	Product size (bp)	Ta (°C)
Chip analysis				
KIAA0367	GTCTTAAGGTGCCATGAGGTTTAG	GATTCATAAGGAAGTCCAGCT	198	58
CADM1 (a)	ACCAGGGAGGAGACCCTC	CAATCTGGGAGAAGTGCATG	216	58
CADM1 (b)	ATTCCCAAGACTGCTCTTCACGCA	AAACTGCACGCCTCTCGTGTTT	338	60
KIAA0895	AGCATTAAGGATAGTATGCTGAGGTAC	GTCTCCAGCCAGTGGGTAAC	249	58
PCDHB14	TTGGTCTCCATCAACGCGGACAAT	CCTTGAGCAGCTGGTACGACA	319	60
UCHL1	GGGTTTCCAGAAACTTCGCCCAAA	CGCCCAGGCTGCAGCTATAAA	289	60
RNF182	AGGGCTCATGGTAGATGCTTAG	GATGTGGTCTCACTCCACCC	212	58
Methylation analysis				
KIAA0367	TATTTTGTAAATGAGTAGTTTTAAGGTGT	AAAATTCATAAAAAAATCCAACTTC	217	58
CADM1 (a)	ATATTAAAATTAGGGAGGAGATTTT	CAAAACAATCTAAAAAAAATACATAC	229	55
CADM1 (b)	TTTGGGTAAATTTTTAAGATTG	ACATCCCCAAACTTATCTAATCT	416	58
KIAA0895	TTAGTATTAAGGATAGTATGTTGAGGTAT	CTAAAATCTCCAACCAATAAATAAC	256	58
PCDHB14	TTTTTAGGGGGTTTTTGTTAAAAAT	AAACCAATTTCTATTTCCTCTACCAC	220	58
UCHL1	AAAAGGATTGTTTTATATATTTAAGGAAT	AAAAAAAACAAAAACAAAACCAAAC	198	58
RNF182	TTTAGGGTTTATGGTAGATGTTTAG	AAATATAATCTCACTCCACCCAAC	216	58

cocktail and sonicated in ice-cold water with a Bioruptor™ (Diagenode, Liège, Belgium) for 13 cycles (30 sec. on – 30 sec. off). Sheared chromatin was centrifuged at 12,000 × *g*, 12 min., 4°C. An aliquot of input DNA was reserved for subsequent positive control. Fragmented DNA was loaded on a gel to visualize the sheared chromatin (average size ~1 kb). ChIP was carried out in siliconized microtubes with the following reagents: Protein G Magnetic Beads, ChIP dilution buffer 1, 6–7 μg of sheared chromatin, 3 μg of the rabbit polyclonal anti-MeCP2 antibody (Millipore Upstate, Molsheim, France) in a total volume of 200 μl. A reaction with a negative control IgG was set up in parallel. Reactions were incubated overnight at 4°C on a rolling shaker. Magnetic beads were then washed and the solutions were reverse cross-linked. Free chromatin was transferred in a new microtube, incubated for 2.5 hrs at 65°C and treated with Proteinase K for 1 hr at 37°C. Proteinase K reaction was stopped and the supernatant containing the eluted DNA was carefully transferred in a clean microtube, prior to PCR analysis.

PCR analysis of ChIP-extracted DNA

CG-rich regions in the close vicinity of our candidate target genes were identified by the Ensembl Genome Browser database, upstream of the +1 transcription initiation site for all genes except *PCDHB14*. In the particular case of the *PCDHB14* gene, which is located at the genomic position chr5:140,583,130–140,586,053, the CpG island that was identified covers the locus chr5:140,584,638–140,585,488, and is indeed fully included within the unique *PCDHB14* coding exon 1. An additional region located in intron 1 was also studied for the *CADM1* gene (Fig. 4A, *CADM1* (b)). PCR amplifications from our regions of interest were carried out using the chromatin collected by the ChIP procedure as a template for the reactions (Table 2). Primers were designed with PrimerQuest℠ from Integrated DNA Technologies website (www.idtdna.com) with default parameters. Each reaction tube was carried out in a final volume of 20 μl and contained 30 ng of either immunoprecipitated or input DNA, 1 U Platinum *Taq* DNA polymerase (Invitrogen), primers 0.5 mM each, dNTPs 0.25 mM each and $MgSO_4$ 1.5 mM. Thermal cycling conditions were: an initial denaturation step at 95°C for 2 min., followed by 35 cycles of 95°C for 30 sec., 58°C or 60°C for 30 sec., with a final extension step of 2 min. for 72°C, in a GeneAmp® PCR 9700 System (Applied Biosystems). PCR products were loaded on an agarose gel stained with ethidium bromide to estimate the enrichment of the specific MeCP2-purified chromatin *versus* the non-specific IgG-purified chromatin of the regions of interest.

DNA methylation analysis

Genomic DNA from a primary culture of normal human fibroblasts was extracted and purified with the Wizard® Genomic DNA Purification Kit (Promega France, Charbonnières-les-Bains, France) and DNA concentration was estimated with the NanoDrop

Table 3 Primer sequences for quantitative RT-PCR

Gene symbol	Accession number	Oligonucleotide sequence (5′-3′)	PCR size (bp)	PCR Ta (°C)
UCHL1	NM_004181	TATGAACTTGATGGACGAATGCC	116	60
		TCTCCTTGCTCACGCTCGGT		
KIAA0367	AB002365	CCACGACATGGAAGAATTTTTG	58	60
		GCGTTTGCTTCGATTCAGTTT		
RNF182	NM_152737	AGCCTGCCCGATGACAAC	57	60
		CTTCCCTTTGCCTCCACAAG		
CADM1	NM_001038558	GGCTTCTGCTGTTGCTCTTC	196	60
		CAACCTCTCCCTCGATCACT		
KIAA0895	NM_015314	ACTGCTCTCGGGAAGGTTTCT	63	60
		TTCGGTAACTGCCAATCCTTTT		
PCDHB14	NM_018934	TTGCACCTTGATTTGCTGAC	106	60
		AAACCACCTGAAAATGCAGC		
PITPNC1	NM_181671	CACAAGGTGGTCCGAGACATT	62	60
		TCATCAACCCATGCAAAAGC		
MECP2	NM_004992	ATCAATCCCCAGGGAAAAGC	70	60
		TGTCGCCTACCTTTTCGAAGTAC		
CPXM2	NM_198148	GTCGCTGGAAGTCTGAACGAT	64	60
		CGTAGATGGACAGTTCGAAGCA		
TNFRSF11B	NM_002546	CTCCAAGCCCCTGAGGTT	96	60
		TCCTGGGTGGTCCACTTAAT		
ITGA4	NM_000885	TTCTACTGGAAGGACTACATC	135	60
		TTTTAAAGAAGCCAGCCTTCC		
SERPINE2	NM_006216	CTGGTTTATAGTAGACAGACC	173	60
		GCAAAGTAGTCGTTGCTTTGC		
ZNF659	NM_024697	GAAAGCAAATCATATCATGCAACAT	62	60
		CGCAGCCTGGCTATCAGAA		
STMN2	NM_007029	ACTGCTCAGCGTCTGCACAT	61	60
		TTTTTTCCTTGTAGGCCATTGC		
GAPDH	NM_002046	GAAGGTGAAGGTCGGAGTC	75	60
		GAAATCCCATCACCATCTTC		

ND-1000 Spectrophotometer. Bisulphite conversion was carried out with the MethylDetector™ kit (Active Motif) according to the manufacturer's protocol. Briefly, 2 μg of pure genomic DNA was incubated with hydroquinone and conversion buffer at 94°C, 3 min. and then at 50°C for 9 hrs. The mixture was loaded on the column provided in the kit, washed, desulfonated and the bisulphite-converted DNA was eluted with 50 μl of DNA elution buffer.

Amplification were carried out in a final volume of 50 μl with 40 ng of bisulphite-converted DNA, 1 U *Taq* DNA polymerase (Invitrogen), 0.5 μM forward and reverse primers (Table 2), dNTP 0.25 mM each, $MgCl_2$ 1.5 mM. Primers were designed with Methyl Primer Express® Software v1.0 (Applied Biosystems) with default parameters. The thermal cycling procedure was: an initial denaturation step at 94°C for 3 min., followed by 40 cycles of 94°C for 30 sec., 55°C or 58°C for 30 sec. and 72°C for 30 sec., with a final extension step of 2 min. at 72°C in a GeneAmp® PCR 9700 System. PCR products were analysed by gel electrophoresis, purified with the QIAquick® PCR Purification kit (Qiagen) and both forward and reverse sequenced with an Applied Biosystems DNA sequencer 3730 (Applied Biosystems) as previously described [19].

Quantitative real-time PCR

Total RNA from the clonal cultures was converted, as described above, to cDNA for quantitative real-time PCR with SYBR Green as

Table 4 Molecular approaches to investigate the clonality of cell cultures from three RTT patients (1, 2 and 3) show discordant results between RT-PCR and XCI analysis. XCI* represents the number of clones showing a total skewed X-chromosome inactivation. For all clones showing no discrepancy between RT-PCR and XCI, immunochemistry confirmed these results

Patient	Age (years old)	Nucleotide change	AA change	Potential clonal cultures	cDNA Sequencing analysis			XCI	
					Wild-type	Mutated	Both	Wild-type	Mutated
1	9	c.C763T	p.R255X	17	5	12	0	1/5 (20%)	5/12 (42%)
2	9	c.C808T	p.R270X	24	18	4	2	3/18 (17%)	2/4 (50%)
3	8	c.1156del41	p.L386HfsX390	15	3	5	7	2/3 (67%)	4/5 (80%)

the detection agent with the ABI Prism 7500 sequence detection system (Applied Biosystems). Primers are described in Table 3. After PCR amplification, a dissociation protocol was performed to determine the melting curve of the PCR product. Reactions with melting curves indicating a single amplification product were considered positive for further analysis. The identity and expected size of the single PCR product were also confirmed by agarose gel electrophoresis. For each cycle, a relative quantification of the amount of each individual gene was calculated by the comparative $\Delta\Delta$CT method as described by the manufacturer (Applied Biosystems), providing a relative measure of the expression of the genes of interest, which were all normalized to the *GAPDH* transcript as the calibrator sample. Statistical analysis was carried out using the nonparametric Mann-Whitney test. A *P*-value <0.05 was considered as significant.

Results

Isolation of wild-type and mutant-MECP2 fibroblast clones

Direct sequencing of the genomic DNA from the three typical RTT patients indicated three different mutations within the *MECP2* gene: two nonsense mutations (p.R255X and p.R270X) and a frameshift mutation (c.1156del41). These are common recurrent mutations known to give rise to RTT. No XCI bias was detected in any of the three studied patients.

MECP2 is an X-linked gene that undergoes XCI in females, so only one *MECP2* allele is expressed from the active X chromosome in each individual cell. Indeed, transcriptome of primary cultures represents genes expressed from cells expressing both the mutated and normal *MECP2* allele. In order to facilitate the identification of differentially expressed genes, we separated the two populations of cells, and carried out single-cell cloning of fibroblasts isolated from skin biopsies. Compared to previous studies [20, 21], we demonstrated the clonality of the selected cells by three independent approaches: *MECP2* mRNA analysis by RT-PCR, X-inactivation status through methylation analysis and immunocytochemistry using antibodies against N- and C-terminal domains of MeCP2. This combined analysis is very important, because discordant results between the RT-PCR analysis and XCI inactivation were observed in many of our potential clones (Table 4). Only clones showing concordant results using the three approaches

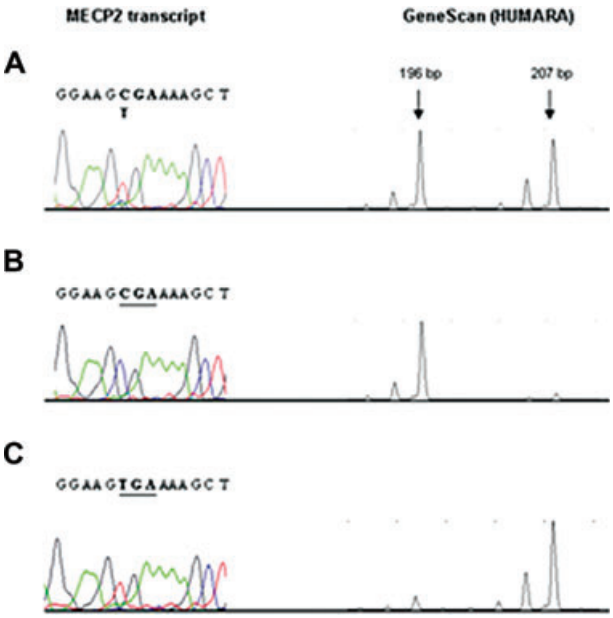

Fig. 1 Results of the molecular approaches used to verify clonality of expanded fibroblasts clones. *MECP2* transcript sequence and GeneScan results for the human androgen receptor (AR) polymorphism used to determined XCI patterns. (**A**) Parental cell strain with p.R255X mutation and mosaic X-inactivation showing the presence of both 196 and 207 bp AR alleles. (**B**) wild-type fibroblast clone from the p.R255X mutation patient, expressing the normal C allele, and carrying the 196 bp AR allele on the inactive X chromosome. (**C**) Mutated fibroblast clone from the p.R255X mutation patient, expressing the mutant T allele, and carrying the 207 bp AR allele on the inactive X chromosome.

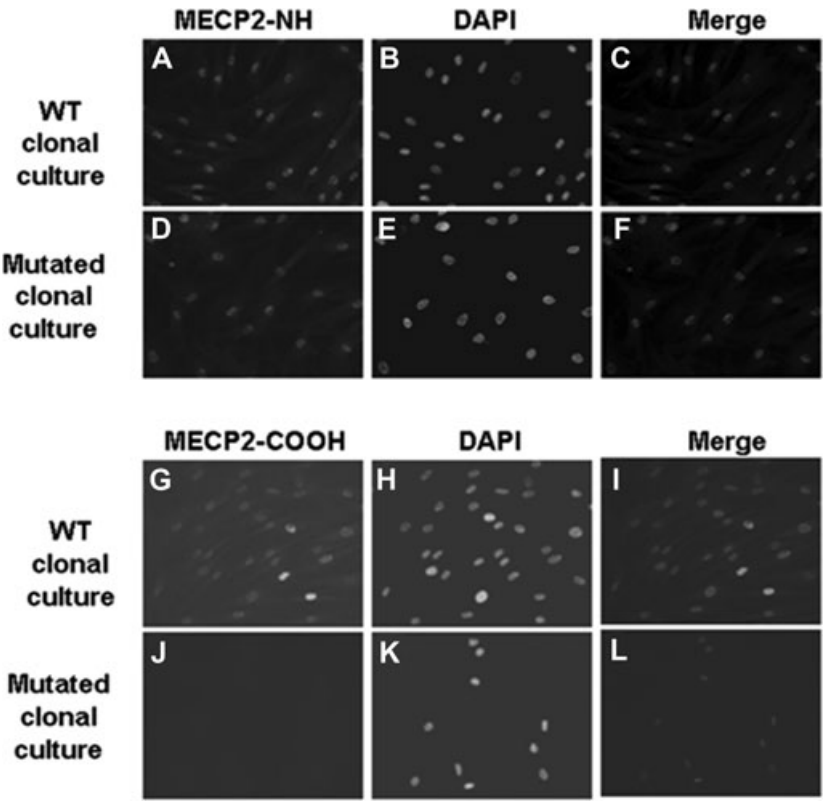

Fig. 2 Immunocytochemical investigations with N-terminal and C-terminal region-specific MeCP2 polyclonal antibodies from clonal fibroblast cultures from a patient with *MECP2* heterozygous for the p.R255X mutation. (**A**), (**B**), (**G**) and (**H**) show wild-type clonal cultures immunostained with DAPI (**B**, **H**) and FITC-conjugated MeCP2 antibody (**A**, **G**). (**D**), (**E**), (**J**) and (**K**) show mutated clonal cultures immunostained with DAPI (**E**, **K**) and FITC-conjugated MeCP2 antibody (**D**, **J**). (**C**), (**F**) and (**I**) represent merged pictures. All wild-type and mutated cells from the patient show positive staining with the antibody against the N-terminal epitope. Cells from mutated clonal cultures show no signal with the antibody against the C-terminal epitope.

were selected for further studies. As illustrated in Figs 1 and 2, all 'clonal' RTT mutant cells, which transcriptome was studied, were (*i*) wild-type transcript-negative, (*ii*) showed complete skewed X-inactivation and (*iii*) expressed truncated mutant proteins.

Microarray analysis of matched fibroblast clones

For each patient, hybridizations of labelled RNA on Human Genome HGU133 Plus2.0 chips were carried out in technical duplicate for each type of clones. Signals of all hybridized chips were normalized using the GC-RMA method. We found that two parameters clearly influenced the analysis by a hierarchical clustering of the microarray data: the genetic background as well as the *MECP2* mutation. Indeed, when comparing wild-type and mutated clones from all RTT patients, clones from one individual tend to cluster together, suggesting the patient background effect (data not shown). To emphasize the *MECP2* mutation effect, mutant clones from RTT patients were compared with mutant clones from atypical RTT subjects bearing a mutation in another gene involved in RTT, *CDKL5*. We observed that the clones cluster in two groups depending on the nature of the mutated gene, while this effect was not observed when wild-type clones were compared, suggesting the *MECP2* mutation-associated effect (data not shown). Therefore, transcriptomic analysis was indeed performed with six clones: one matched pair (one mutant and one wild-type clones) from each of the three *MECP2* mutation patients. When several wild-type or mutant clones were available from the same patient, the one presenting the closest 100:0 skewed X-inactivation score was selected for the transcriptomic analysis. One mutant and one wild-type clone from each individual were first compared (paired t-test). Microarray data have been submitted into the ArrayExpress database (www.ebi.ac.uk/aerep/login; Username: Reviewer_E-MEXP-1956, and Password: 1229698048509). *R*-paired t-test analysis, considering a $P < 0.05$ and a 2-fold expression variation, yielded a total of 27 genes with significantly different expression between wild-type and mutant samples. Of these, 11 had an increased level of expression and 16 had a reduced level of expression (Table 5). In a second set of experiments, all mutant clones were compared with all wild-type clones (unpaired t-test). This statistical analysis indicated 20 differentially expressed genes. Twelve genes were overexpressed and eight were underexpressed in mutant clones compared to wild-type clones. Another unpaired statistical analysis with Genespring found 11 overexpressed genes and 10 underexpressed genes in mutant clones compared to wild-type clones (Table 5). Taken together, a total of 22 genes were statistically up-regulated in at least one statistical analysis, and 22 other were down-regulated. Nine of these were significantly dysregulated in all statistical analyses.

We focused our study on the differentially expressed genes highlighted by all statistical analyses: four overexpressed genes (*KIAA0367*, *CADM1*, *KIAA0895*, *PCDHB14*) and five underexpressed

Table 5 Genes with higher expression (>2 fold change in expression level) and with lower expression (<0.5 fold change in expression level) in mutant samples on microarray analysis. This table contains the list of genes significantly dysregulated in at least one of the three statistical analysis (paired-t-Test; unpaired-t-Test, and Genespring) ($P < 0.05$). ns: not significant

Gene Symbol	Gene name	Accession number	Fold change (MECP2 mutated over WT)	Paired t-Test *P*-value	Unpaired t-Test *P*-value	GeneSpring *P*-value
UCHL1	Ubiquitin carboxyl-terminal esterase L1 (ubiquitin thiolesterase)	NM_004181	10.77	ns	ns	0.027
DSP	Desmoplakin	NM_004415	8.90	0.012	ns	ns
KIAA0367	KIAA0367	AB002365	7.96	0.002	0.001	0.001
RNF182	Ring finger protein 182	NM_152737	7.61	ns	ns	0.028
CADM1	Cell adhesion molecule 1 precursor	NM_001038558	3.98	0.048	0.004	0.039
MASK	Mst3 and SOK1-related kinase	AB040057	3.39	0.033	ns	ns
DOK5	Docking protein 5	NM_018431	3.32	ns	0.025	ns
SPG3A	Spastic paraplegia 3A	NM_015915	3.16	0.042	ns	ns
EDN1	Endothelin 1	NM_001955	2.98	0.014	0.027	ns
GDF5	Growth differentiation factor 5 (cartilage-derived morphogenetic protein-1)	NM_000557	2.62	ns	0.045	ns
LOC401022	Hypothetical LOC401022	BC047481	2.48	ns	0.032	0.038
KIAA0895	KIAA0895 protein	NM_015314	2.46	0.017	0.004	0.001
PTGER3	Prostaglandin E receptor 3 (subtype EP3)	NM_000957	2.45	0.007	ns	ns
ANXA1	Annexin A1	NM_000700	2.43	ns	ns	0.043
SRPX2	Sushi-repeat-containing protein, X-linked 2	NM_014467	2.35	ns	ns	0.045
PCDHB14	Protocadherin β_{14}	NM_018934	2.26	0.038	0.047	0.022
HOXD3	Homeo box D3	NM_006898	2.23	0.011	0.028	ns
BHMT2	Betaine-homocysteine methyltransferase 2	NM_017614	2.21	ns	0.047	0.049
FOLR3	Folate receptor 3 (γ)	NM_000804	2.21	ns	0.034	ns
SEMA6D	Sema domain, transmembrane domain (TM), and cytoplasmic domain, (semaphorin) 6D	NM_020858	2.18	ns	0.050	ns
STC2	Stanniocalcin 2	NM_003714	2.15	ns	ns	0.047
PSG9	Pregnancy specific β_1-glycoprotein 9	NM_002784	2.04	0.050	ns	ns
Gene Symbol	**Gene name**	**Accession number**	**Fold change (MECP2 mutated over WT)**	**Paired t-Test *P*-value**	**Unpaired t-Test *P*-value**	**GeneSpring *P*-value**
PITPNC1	Phosphatidylinositol transfer protein, cytoplasmic 1	NM_181671	0.50	ns	ns	0.037
PLCL2	Phospholipase C-like 2	NM_015184	0.49	0.028	ns	ns
BNC1	Basonuclin 1	NM_001717	0.48	0.044	ns	ns
PCDH18	Protocadherin 18	NM_019035	0.48	0.029	ns	ns
GREM2	Gremlin 2, cysteine knot superfamily, homolog (Xenopus laevis)	NM_022469	0.46	0.023	ns	ns

Continued

Table 5 Continued.

Gene Symbol	Gene name	Accession number	Fold change (MECP2 mutated over WT)	Paired t-Test *P*-value	Unpaired t-Test *P*-value	GeneSpring *P*-value
SSPN	Sarcospan (Kras oncogene-associated gene)	NM_005086	0.46	0.004	ns	ns
MECP2	Methyl CpG binding protein 2 (RTT)	NM_004992	0.46	0.015	0.008	0.013
TCF8	Transcription factor 8 (represses interleukin 2 expression)	AK314683	0.45	0.019	ns	ns
PPAP2B	Phosphatidic acid phosphatase type 2B	NM_177414	0.44	0.024	ns	ns
CPXM2	Carboxypeptidase X (M14 family), member 2	NM_198148	0.42	ns	0.025	0.009
EMP2	Epithelial membrane protein 2	NM_001424	0.39	0.042	0.013	ns
CHN1	Chimerin (chimaerin) 1	NM_001822	0.39	ns	0.031	ns
TNFRSF11B	Tumor necrosis factor receptor superfamily, member 11b (osteoprotegerin)	NM_002546	0.39	0.047	0.049	0.011
ASPA	Aspartoacylase (Canavan disease)	NM_001128085	0.38	ns	ns	0.047
EPB41L3	Erythrocyte membrane protein band 4.1-like 3	NM_012307	0.38	0.029	ns	ns
ITGA4	Integrin, α_4 (antigen CD49D, α_4 subunit of VLA-4 receptor)	NM_000885	0.36	0.033	0.031	0.049
SERPINE2	Serpin peptidase inhibitor, clade E (nexin, plasminogen activator inhibitor type 1), member 2	NM_006216	0.36	0.027	0.036	0.007
ZNF659	Zinc finger protein 659	NM_024697	0.34	0.022	0.006	0.039
SLC1A3	Solute carrier family 1 (glial high affinity glutamate transporter), member 3	NM_004172	0.33	0.013	ns	ns
ITGA6	Integrin, α_6	NM_001079818	0.29	0.037	ns	ns
ENPP1	Ectonucleotide pyrophosphatase/ phosphodiesterase1	NM_006208	0.25	ns	ns	0.013
STMN2	Stathmin-like 2	NM_007029	0.08	ns	ns	0.029

genes (*MECP2*, *ITGA4*, *TNFRSF11B*, *SERPINE 2*, *ZNF659*), as well as five candidate genes that have been also previously identified in other studies (*UCHL1*, *PITPNC1*, *RNF182*, *CPXM2* and *STMN2*) [6, 21–23].

Expression study of our selected target genes by quantitative RT-PCR was carried out both with the same clones as for the transcriptomic analysis, and with the other validated clones (one additional wild-type and one mutated clones for c.1156del41 and p.R270X, and only one mutated for p.R255X). The results confirmed that *CADM1*, *KIAA0367*, *RNF182*, *UCHL1*, *KIAA0895*, *PCDHB14* are up-regulated in all human mutant MeCP2 fibroblasts while *TNFRSF11B*, *PITPNC1*, *SERPINE2*, *CPXM2*, *ZNF659*, *ITGA4* and *STMN2* are down-regulated (Fig. 3).

ChIP and bisulphite-converted DNA sequencing of up-regulated target genes

To determine whether MeCP2 directly binds to the potential overexpressed target genes, we carried out ChIP assays using a normal human fibroblast cell culture and either an anti-MeCP2 antibody or a control IgG antibody. The immunoprecipitated chromatin was used as a template for subsequent amplifications of CpG-rich domains found in the close vicinity of our candidate genes except for *PCDHB14* where the CpG island is located within exon 1 (Fig. 4A). Several targets were shown to be relatively enriched with the anti-MeCP2 antibody as compared with the negative control IgG: *KIAA0367*, *PCDHB14*, *RNF182* and *CADM1* (Fig. 4B). For genes such as *KIAA0895* and, *UCHL1*, our results suggest that MeCP2-related complex does not bind to the promoter regions of these genes. Although our statistical analysis did not highlight that *UCHL1* was regulated by MeCP2 in all set of experiments (Table 5), it is not excluded that MeCP2 may bind outside the targeted regions, or MeCP2 deficiency may indirectly alter *UCHL1* expression. Alternatively, the effect of MeCP2 on gene expression may involve long-range chromatin interactions [14].

As MeCP2 function depends, but not exclusively, on its binding to methylated CpGs [14], we tested CpG methylation by sequencing bisulphite-converted genomic DNA extracted from human fibroblasts. Regions of interest were designed to overlap with the

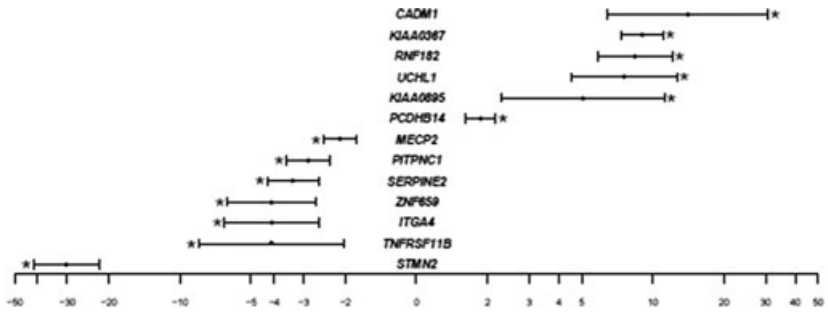

Fig. 3 Quantitative RT-PCR (qRT-PCR) analysis of MeCP2 target gene expression. The *X*-axis shows the log2 gene expression average ratios (±S.D.) of mutant compared to wild-type. Asterisk indicates a *P*-value <0.05.

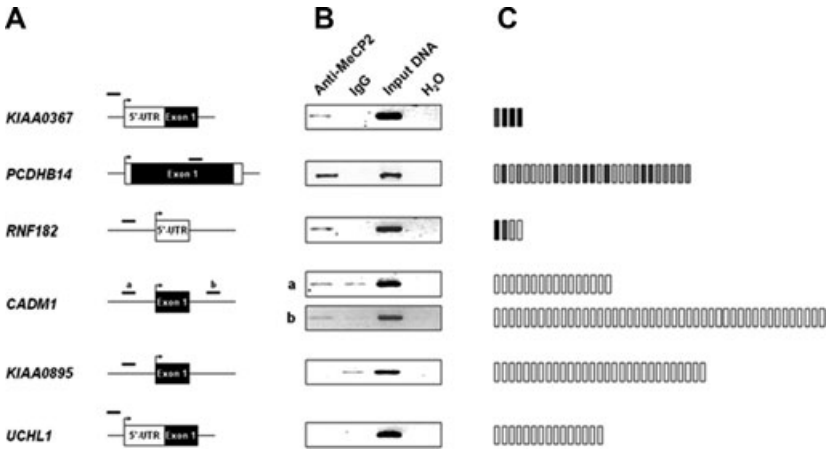

Fig. 4 Analysis of MeCP2 binding to CpG-methylated regions in the vicinity of putative target genes in a primary culture of human fibroblasts. (**A**) Schematic representation of the position of regions (black lines above schemes, respectively) amplified after ChIP byananti-MeCP2 antibody. Two regions, respectively referred to as 'a' and 'b', were studied in the vicinity of *SGSF4*. (**B**) PCR amplification profiles. DNA and proteins were cross-linked and precipitated with an anti-MeCP2 antibody orpreimmune IgG as a control. After reverse cross-linking, DNA was PCR amplified and the products were loaded on a gel. Input DNA was amplified as positive control. (**C**) Schematic representation of DNA methylation profiles after bisulphite conversion of genomic DNA. White squares represent unmethylated CpGs (0%), black squares are methylated CpGs (100%), and grey squares are partially methylated CpGs.

sequences amplified after ChIP. Several methylated CpG sites were observed in the vicinity of *KIAA0367*, *PCDHB14* and *RNF182* genes (Fig. 4C), which are also all immunoprecipitated by MeCP2. These results are compatible with the hypothesis that MeCP2 is involved in the repression of *KIAA0367*, *PCDHB14* and *RNF182* genes. Absence of identification of methylated CpG sites in the promoter regions of *CADM1* could be explained by the recent observation that the majority of MeCP2 binding sites were found outside of transcription units and CpG islands [7].

Discussion

Mutations in the X-linked *MECP2* gene are found in most girls with RTT at the heterozygous state. The *MECP2* gene is subjected to XCI and classic RTT patients typically exhibit random XCI patterns. Hence, patients with RTT have a mosaic distribution of cells expressing either the wild-type or the mutant *MECP2* allele in their tissues. Analysis of gene expression profiles in tissues from girls with RTT will therefore be compromised by unpredictable patterns of XCI. In addition, the presence of functional wild-type cells will also dilute the effects of abnormal expression level of MeCP2 target genes. Although the brain is the most severely affected tissue in RTT, one might argue that expression studies in human from total brain tissue are not the most accessible and appropriate models to implement. Firstly, samples from live human patients are obviously unavailable. Studies using post-mortem tissues have been performed but the samples have mostly originated from girls at late stages of the disorder and their expression profiles may reflect the pathogenesis of concurrent disease [24]. Secondly, expression changes could be interpreted as a secondary effect of the disease process, such as increased expression of glial-specific genes and decreased expression of neuronal genes [24]. Finally, the brain is a very complex tissue characterized by a large cell heterogeneity that could dilute the effect of MeCP2 deficiency. Because neurons from the central nervous system are the primary cell types in which the pathology occurs, a pure population of neurons would constitute an ideal sample set for the analysis of gene expression profiles in *MECP2*-deficient cells. Unfortunately, such samples are unavailable and alternative strategies are required.

MeCP2 is virtually expressed in all tissues, including skin. Fibroblast cells were isolated and clonally expanded in order to compare *MECP2* wild-type and mutant transcript expression originated from the same individual. Because only a single *MECP2* allele is expressed in each clone, we expected that effects on gene

expression profiles would be highlighted. Furthermore, by comparing these clonal cells, we eliminated interindividual variations resulting from genetic background from one patient to another. Delgado and colleagues experimented a similar approach with T-lymphocytes [21], and Traynor and colleagues studied lymphoblastoid cell lines and fibroblast clones [15]. The main drawback of lymphoblastoid cells is that immortalization can affect gene expression patterns. To prevent from epigenetic differences because fibroblasts divide in cultures (as previously described using the fibroblasts from Coriell repository) [15], primary cultures of untransformed fibroblasts with a low number of cell divisions were chosen for our study. Moreover, we made sure that all selected clones had a normal 46,XX caryotype.

Given that all analysed *MECP2* mutations are non-sense or frameshift likely to be associated with highly unstable transcripts, it is of interest to note that the underexpression of MeCP2, detected in all statistical analysis, validated our matched pairs of cell clones (wild-type *versus* mutant) as a useful experimental system for the investigation of MeCP2 deficiency downstream effects. These results are in accordance with previous data showing that the truncating mutations (non-sense and frameshift) are significantly associated with lower levels of both *MECP2* isoforms (MECP2_e1 and MECP2_e2) compared to normal controls and patients bearing non-truncating mutations (missense and inframe) [25].

In the study by Traynor *et al.*, the authors analysed four fibroblast strains obtained from Coriell Cell repositories carrying different classes of mutations (missense mutations: p.R106W, p.R306C and frameshift mutations: c.705delG, c.1155del32) [15]. Surprisingly, in this study, the level of *MECP2* transcript was virtually identical as determined by real-time quantitative RT-PCR analysis in all wild-type and mutated clones. Therefore, assessment of clonality by different approaches is a very critical parameter because we have clearly shown discordance between the different molecular and cellular approaches in several wild-type and mutated clones, which were not suitable for transcriptomic analysis. In some potential clones, which were not selected in our transcriptomic analysis, we only observed a mono-allelic expression of *MECP2* transcript although X-inactivation status was random. Such discordance between methylation status and transcript expression have been also previously reported [26]. Though mechanisms underlying this discordance remain to be further investigated, recent studies have shown that at least 1000 autosomal human genes are subjected to random monoallelic expression [27]. Similarly, we suggest that random deregulation of methylation in clonal cell cultures might be the basis of the observed discrepancy.

Our data compared with others published in the literature display very limited overlap. One down-regulated gene, *PITPNC1*, encoding the phosphatidylinositol transfer protein, was also found to be down-regulated by Delgado *et al.* in mutant T-lymphocyte clones [21]. In another study, microarray-based global gene expression studies in cerebellum of mutant Mecp2 mice ($Mecp2^{tm1.1Jae}$ and $Mecp2^{tm1.1Bird}$) identified the *Stmn2* gene as underexpressed [22]. *Uchl1*, encoding the ubiquitin carboxyterminal hydrolase L1, was also identified as an overexpressed gene ($\times$1.53) in hippocampal granule neurons of $Mecp2^{tm1.1Jae}$ KO mice [23]. Moreover, five of the differentially expressed genes identified in our study (*RNF182*, *CADM1*, *ITGA4*, *CPXM2*, *STMN2*) have been identified as misregulated in the hypothalami from Mecp2 null mice and/or Mecp2-Tg mice [6]. In both studies, *CPXM2*, *STMN2*, *ITGA4* are down-regulated in Mecp2-deficient cells, while *RNF182* and *CADM1* are up-regulated in Mecp2-deficient cells or down-regulated in Mecp2-overexpressing cells (Mecp2-Tg) [6]. Because the expression of *CADM1*, *ITGA4* and *STMN2* was only altered in a single mouse model, the authors suggested that they likely represent secondary changes due to either altered expression of primary gene targets of MeCP2 or disease process.

The limited overlap of genes identified with up- or down-regulated expression between the different studies may have several reasons: study of different tissues/cell lines, class of mutations, human *versus* mouse samples, as well as stages of the disease. For an accurate comparison, our three unrelated patients had a convergent, classical RTT phenotype and a similar age (8–9 years old). An alternate hypothesis is that MeCP2 primarily regulates the expression of a limited number of genes in very specific cells or in a transient manner.

Although the global level of gene expression is not significantly altered, it does not preclude the possibility that some of the genes may have subtle expression variations that are biologically relevant. Moreover, although we studied non-neuronal cells, we identified differentially expressed genes that are functionally relevant in brain (such as *KIAA0367*), especially in neurons. Recently, it has been shown that *KIAA0367* corresponds to *BMCC1* (Bcl-2, the adenovirus E1B 19 kD interacting protein 2 (BNIIP2) and the Cdc42 GAP homology BCH motif-containing molecule at the carboxy terminal region 1). This gene encodes a large protein expressed in many tissues, and highly expressed in the nervous system (brain, cerebellum and spinal cord) as well as in adrenal gland. The level of *BMCC1* mRNA is modulated during neuronal differentiation and apoptosis in an opposite manner, and *BMCC1* overexpression may function as an inducible pro-apoptotic signal in neuronal cells [28]. Our results may partially explain the recent observation in mutant mouse models suggesting that the loss of MeCP2 function or its complete knockdown induces a death program at an earlier time period after hypoxia and excitotoxicity in cerebellar granule neurons in both caspase- and AIF-dependent manners. Considering that MeCP2 inactivation may repress gene expression or result in a transcriptional dysregulation, it is conceivable that overexpression of pro-death component molecules, such as BMCC1, fragilizes the neurons that become more vulnerable to injury and death [29]. Moreover, it has been shown that activated TrkA physically interacts with BMCC1, which in turn regulates the downstream signalling to control growth, differentiation and survival of neuronal cells. Interestingly, expression of TrkA is significantly reduced in brain of RTT patients [30].

Another interesting target gene is *CADM1*. The product of the gene is an immunoglobulin-like intercellular, adhesion molecule that plays a critical role in the telencephalon and cerebellum development [31]. Moreover, this gene is localized in an interval in which a small 11q23.3 *de novo* duplication has been associated with atypical RTT in a girl [32].

A third target gene is *PCDHB14*. This single-exon gene is one of the 16 randomly arranged genes in the PCDH-β gene cluster on chromosome 5q31. It encodes the extracellular, transmembrane, short cytoplasmic domains of a calcium-dependent cell–cell adhesion protein [33]. Although the biological role of PCDHB14 is unknown, members of this protocadherin family are predominantly expressed in the nervous system and are thought to be involved in the establishment of neuronal connections and in signal transduction at the synaptic membrane [34]. Expression studies in the mouse adult brain showed that *PCDHB14* is expressed in the hippocampus and the cerebellum (http://www.brain-map.org). The relevance of our data is reinforced by the recent involvement of *PCDH19* in epilepsy and intellectual disability [35].

The last interesting target gene is *RNF182*, which encodes a RING-finger-containing transmembrane protein. Previous quantitative RT-PCR analysis indicated that this gene is detected in the mouse cortex, hippocampus, cerebellum and spinal cord, and is expressed in differentiated neurons and astrocytes [36]. It is of interest to note that *RNF182* (Unigene Hs.111164) was first identified as up-regulated in a previous comparison of mutant/wild-type human fibroblast clones [15]. Moreover, it has been shown that *RNF182* is up-regulated in Alzheimer's disease brain and in neuronal cells subjected to stress-induced cell death. Its overexpression in N2A cells triggered cell death by itself [36]. Although cell death does not play a major role in the alteration or maintenance of cell homeostasis during development of MeCP2$^{308/y}$ mouse, it has been observed that by 52 weeks, the strategy of increasing neuronal precursors to maintain a population of mature cells fails and apoptosis increases [37].

In line with previous studies, our transcriptional profiling using fibroblast clones expressing exclusively either the mutated or the wild-type *MECP2* allele revealed significant subtle changes in MeCP2 human cells. We identified both previously reported and novel direct MeCP2 target genes by showing an increased expression and binding of MeCP2 to their methylated promoters. The most interesting genes appears to be *KIAA0367* (*BMCC1*), *PCDHB14*, *CADM1* and *RNF182*, which are all expressed in the brain. Some of these target genes (such as *KIAA0367* [*BMCC1*], *CADM1*, *RNF182* and *STMN2*) are directly or indirectly involved in the regulation of the cell growth and survival of neuronal cells [38] and these results provide new insights into the mechanisms underlying postnatal neurodevelopmental abnormalities associated with RTT. To evaluate the contributions of these misregulated genes to the synaptic dysfunction and neuropathological phenotype observed in MeCP2-deficient human cells, further studies in mouse models, as well as genetic interaction studies, siRNA and functional assays of the affected pathways will be required.

Acknowledgements

We thank the families for participating, especially the members of the Association Française du Syndrome de Rett (AFSR). We also thank Yoann Saillour for excellent technical assistance. This work was supported by Institut National de la Santé et de Recherche Médicale (ANR-Maladies Rares ANR-06-MRAR-003-01; ANR-08-e-rare) and Fondation de la Recherche Médicale (FRM). HRV has a postdoctoral fellowship from the Instituto Mexicano del Seguro Social (IMSS) and JN is supported by the Fondation de la Recherche Médicale (FRM).

References

1. **Amir RE, Van den Veyver IB, *et al.*** Rett syndrome is caused by mutations in X-linked MECP2, encoding methyl-CpG-binding protein 2. *Nat Genet.* 1999; 23: 185–8.
2. **Bienvenu T, Chelly J**. Molecular genetics of Rett syndrome: when DNA methylation goes unrecognized. *Nat Rev Genet*. 2006; 7: 415–26.
3. **Klose RJ, Sarraf SA, Schmiedeberg L, *et al.*** DNA binding selectivity of MeCP2 due to a requirement for A/T sequences adjacent to methyl-CpG. *Mol Cell*. 2005; 19: 667–78.
4. **Nan X, Tate P, Li E, *et al.*** DNA methylation specifies chromosomal localization of MeCP2. *Mol Cell Biol*. 1996; 16: 414–21.
5. **Nan X, Ng HH, Johnson CA, *et al.*** Transcriptional repression by the methyl-CpG-binding protein MeCP2 involves a histone deacetylase complex. *Nature*. 1998; 393: 386–9.
6. **Chahrour M, Jung SY, Shaw C, *et al.*** MeCP2, a key contributor to neurological disease, activates and represses transcription. *Science. 2008;* 320: 1224–9.
7. **Yasui DH, Peddada S, Bieda MC, *et al.*** Integrated epigenomic analyses of neuronal MeCP2 reveal a role for long-range interaction with active genes. *Proc Natl Acad Sci USA*. 2007; 104: 19416–21.
8. **Tudor M, Akbarian S, Chen RZ, *et al.*** Transcriptional profiling of a mouse model for Rett syndrome reveals subtle transcriptional changes in the brain. *Proc Natl Acad Sci USA*. 2002; 99: 15536–41.
9. **Chen WG, Chang Q, Lin Y, *et al.*** Derepression of BDNF transcription involves calcium-dependent phosphorylation of MeCP2. *Science*. 2003; 302: 885–9.
10. **Martinowich K, Hattori D, Wu H, *et al.*** DNA methylation-related chromatin remodeling in activity-dependent BDNF gene regulation. *Science*. 2003; 302: 890–93.
11. **Makedonski K, Abuhatzira L., Kaufman Y, *et al.*** MeCP2 deficiency in Rett syndrome causes epigenetic aberrations at the PWS/AS imprinting center that affects UBE3A expression. *Hum Mol Genet*. 2005; 14: 1049–58.
12. **Horike S, Cai S, Miyano M, *et al.*** Loss of silent chromatin looping and impaired imprinting of DLX5 in Rett syndrome. *Nat Genet*. 2005; 37: 31–40.
13. **Schüle B, Li HH, Fisch-Kohl C, *et al.*** DLX5 and DLX6 expression is biallelic and not modulated by MeCP2 deficiency. *Am J Hum Genet*. 2007; 81: 492–506.
14. **Chahrour M, Zoghbi HY**. The story of Rett syndrome: from clinic to neurobiology. *Neuron*. 2007; 56: 422–37.
15. **Traynor J, Agarwal P, Lazzeroni L, *et al.*** Gene expression patterns vary in clonal cell cultures from Rett syndrome females with eight different MECP2 mutations. *BMC Med Genet*. 2002; 3: 12.

16. **Allen RC, Zoghbi HY, Moseley AB, *et al.*** Methylation of HpaII and HhaI sites near the polymorphic CAG repeat in the human androgen-receptor gene correlates with X chromosome inactivation. *Am J Hum Genet.* 1992; 51: 1229–39.
17. **Lasalle JM, Goldstine J, Balmer D, *et al.*** Quantitative localization of heterogeneous methyl-CpG-binding protein 2 (MeCP2) expression phenotypes in normal and Rett syndrome brain by laser scanning cytometry. *Hum Mol Genet.* 2001; 10: 1729–40.
18. **Irizarry RA, Wu Z, Jaffee HA**. Comparison of Affymetrix genechip expression measures. *Bioinformatics.* 2006; 22: 789–94.
19. **Ballestar E, Ropero S, Alaminos M, *et al.*** The impact of MECP2 mutations in the expression patterns of Rett syndrome patients. *Hum Genet.* 2005; 116: 91–104.
20. **Balmer D, Arredondo J, Samaco RC, *et al.*** MECP2 mutations in Rett syndrome adversely affect lymphocyte growth, but do not affect imprinted gene expression in blood or brain. *Hum Genet.* 2002; 110: 545–52.
21. **Delgado IJ, Kim DS, Thatcher KN, *et al.*** Expression profiling of clonal lymphocyte cell cultures from Rett syndrome patients. *BMC Med Genet.* 2006; 21: 61.
22. **Jordan C, Li HH, Kwan HC, *et al.*** Cerebellar gene expression profiles of mouse models for Rett syndrome reveal novel MeCP2 targets. *BMC Med Genet.* 2007; 8: 36.
23. **Smrt RD, Eaves-Egenes J, Barkho BZ, *et al.*** Mecp2 deficiency leads to delayed maturation and altered gene expression in hippocampal neurons. *Neurobiol Dis.* 2007; 1: 77–89.
24. **Colantuoni C, Jeon H, Hyde K, *et al.*** Gene expression profiling in postmortem Rett Syndrome braindifferential gene expression and patient classification. *Neurobiol Dis.*2001; 8: 847–65.
25. **Petel-Galil Y, Benteer B, Galil YP, *et al.*** Comprehensive diagnosis of Rett's syndrome relying on genetic, epigenetic and expression evidence of deficiency of the methyl-CpG-binding protein 2 gene: study of a cohort of Israeli patients. *J Med Genet.* 2006; 43: e56.
26. **El Kassar N, Hetet G, Brière J, *et al.*** X-chromosome inactivation in healthy females: incidence of excessive lyonization with age and comparison of assays involving DNA methylation and transcript polymorphisms. *Clin Chem.* 1998; 44: 61–7.
27. **Gimelbrant A, Hutchinson JN, Thompson BR, *et al.*** Widespread monoallelic expression on human autosomes. *Science.* 2007; 318: 1136–40.
28. **Machida T, Fujita T, Ooo ML, *et al.*** Increased expression of proapoptotic BMCC1, a novel gene with the BNIP2 and Cdc42GAP homology (BCH) domain, is associated with favorable prognosis in human neuroblastomas. *Oncogene.* 2006; 25: 1931–42.
29. **Russell JC, Blue ME, Johnston MV, *et al.*** Enhanced cell death in MeCP2 null cerebellar granule neurons exposed to excitotoxicity and hypoxia. *Neuroscience.* 2007; 150: 563–74.
30. **Lipani JD, Bhattacharjee MB, Corey DM, *et al.*** Reduced nerve growth factor in Rett syndrome postmortem brain tissue. *J Neuropathol Exp Neurol.* 2000; 59: 889–95.
31. **Ohta Y, Itoh K, Yaoi T, *et al.*** Spatiotemporal patterns of expression of IGSF4 in developing mouse nervous system. *Brain Res Dev Brain Res.* 2005; 156: 23–31.
32. **Delobel B, Delannoy V, Pini G, *et al.*** Identification and molecular characterization of a small 11q23.3 *de novo* duplication in a patient with Rett syndrome manifestations. *Am J Med Genet.* 1998; 80: 273–80.
33. **Wu Q, Zhang T, Cheng JF, *et al.*** Comparative DNA sequence analysis of mouse and human protocadherin gene clusters. *Genome Res.* 2001; 11: 389–404.
34. **Yagi T, Takeichi M**. Cadherin superfamily genes: functions, genomic organization, and neurologic diversity. *Genes Dev.* 2000; 14: 1169–80.
35. **Dibbens LM, Tarpey PS, Hynes K, *et al.*** X-linked protocadherin 19 mutations cause female-limited epilepsy and cognitive impairment. *Nat Genet.* 2008; 6: 776–81.
36. **Liu QY, Lei JX, Sikorska M, *et al.*** A novel brain-enriched E3 ubiquitin ligase RNF182 is up regulated in the brains of Alzheimer's patients and targets ATP6V0C for degradation. *Mol Neurodegeneration.* 2008; 3: 1–16.
37. **Palmer A, Qayumi J, Ronnett G**. MeCP2 mutation causes distinguishable phases of acute and chronic defects in synaptogenesis and maintenance, respectively. *Mol Cell Neurosci.* 2008; 37: 794–807.
38. **Bahn S, Mimmack M, Ryan M, *et al.*** Neuronal target genes of the neuron-restrictive silencer factor in neurospheres derived from fetuses with Down's syndrome: a gene expression study. *The Lancet.* 2002; 359: 310–5.